

Escape driven by strongly correlated noise

Peter Hänggi, Peter Jung, Fabio Marchesoni

Angaben zur Veröffentlichung / Publication details:

Hänggi, Peter, Peter Jung, and Fabio Marchesoni. 1989. "Escape driven by strongly correlated noise." *Journal of Statistical Physics* 54 (5-6): 1367–80.
<https://doi.org/10.1007/BF01044720>.



Escape Driven by Strongly Correlated Noise

Peter Hänggi,¹ Peter Jung,¹ and Fabio Marchesoni^{1,2}

We consider the colored-noise-driven archetypal bistability dynamics of the Ginzburg–Landau type. The focus is on the stationary behavior and the problem of escape from metastable states. The deterministic flow of the underlying *two-variable* Fokker–Planck process is studied as a function of the noise correlation time τ . As a main result we find that the separatrix exhibits a cusp at asymptotically large noise color. The stationary probability is evaluated approximately (unified colored noise approximation) and compared with numerical exact results. The stationary probability forms the key input in the evaluation of the rate of escape. At very strong noise color, the escape path closely follows a nodal line, passing through the corresponding stable node. The asymptotic result for the escape rate at large τ is compared with exact calculations for the lowest, nonvanishing eigenvalue.

1. INTRODUCTION

The inclusion of realistic noise sources with a finite correlation time in modeling dynamical systems is attracting rapidly growing interest.^(1,2) In particular, it has been recognized that the finite correlation time of the environmental noise can impact both the stationary and the dynamic features of a nonlinear system.^(1–3) For example, taking the large class of metastable *thermal equilibrium* systems, it has been demonstrated that memory friction or, via the fluctuation dissipation theorem, colored thermal noise can substantially modify the classical, diffusive barrier transmission (see ref. 4 for a survey of the state of the art).⁽⁵⁾

¹ University of Augsburg, D-8900 Augsburg, West Germany.

² Dipartimento di Fisica dell'Università and Istituto Nazionale di Fisica Nucleare, I-06100 Perugia, Italy.

The situation is even more difficult in *stationary nonequilibrium* systems that generally do not obey the condition of manifest detailed balance.^(6,7) The archetypal situation is a nonequilibrium Ginzburg–Landau-type bistable dynamics pioneered in ref. 7. Let us consider the symmetric bistable flow

$$\dot{x} = ax - bx^3 + \varepsilon(t), \quad a > 0, \quad b > 0 \tag{1.1}$$

driven by exponentially correlated Gaussian noise

$$\langle \varepsilon(t) \varepsilon(s) \rangle = \frac{D}{\tau} \exp\left(-\frac{1}{\tau} |t - s|\right) \tag{1.2}$$

Here, τ is the noise correlation time and D denotes the noise intensity. Throughout the following sections we shall use dimensionless variables only, i.e., $x \rightarrow (b/a)^{1/2} x$, $\varepsilon \rightarrow (b/a^3)^{1/2} \varepsilon$, $t \rightarrow at$, which obey (1.1) with $a = b = 1$ and dimensionless noise intensity $D \rightarrow Db/a^2$ and correlation time $\tau \rightarrow a\tau$.

The non-Markovian flow in (1.1) can be embedded into a two-dimensional Markovian process, i.e.⁽⁷⁾

$$\dot{x} = x - x^3 + \varepsilon \tag{1.3a}$$

$$\dot{\varepsilon} = -\frac{1}{\tau} \varepsilon + \frac{D^{1/2}}{\tau} \xi(t) \tag{1.3b}$$

with $\xi(t)$ being a white Gaussian noise; i.e., $\langle \xi(t) \rangle = 0$, $\langle \xi(t) \xi(s) \rangle = 2\delta(t - s)$. In showing the equivalence with (1.1) we prepare $\varepsilon(t)$ according to the stationary Gaussian probability

$$\bar{\rho}(\varepsilon) = \left(\frac{\tau}{2\pi D}\right)^{1/2} \exp\left(-\frac{\tau\varepsilon^2}{2D}\right)$$

2. DETERMINISTIC FLOW

In the absence of noise, the deterministic dynamics is given by

$$\dot{x} = x - x^3 + \varepsilon, \quad \dot{\varepsilon} = -\varepsilon/\tau \tag{2.1}$$

Equation (2.1) is symmetric under reflection, i.e., $x \rightarrow -x$, $\varepsilon \rightarrow -\varepsilon$, and has three fixed points, two locally stable fixed points at $x = \pm 1$, $\varepsilon = 0$ (stable nodes) and an unstable fixed point at $x = 0$, $\varepsilon = 0$ (saddle point). In Fig. 1 we depict the deterministic flow for various correlation times: (a) $\tau = 0.2$, (b) $\tau = 10$, (c) $\tau = 30$. The separatrix $\varepsilon_s(x; \tau)$ dividing the two basins of

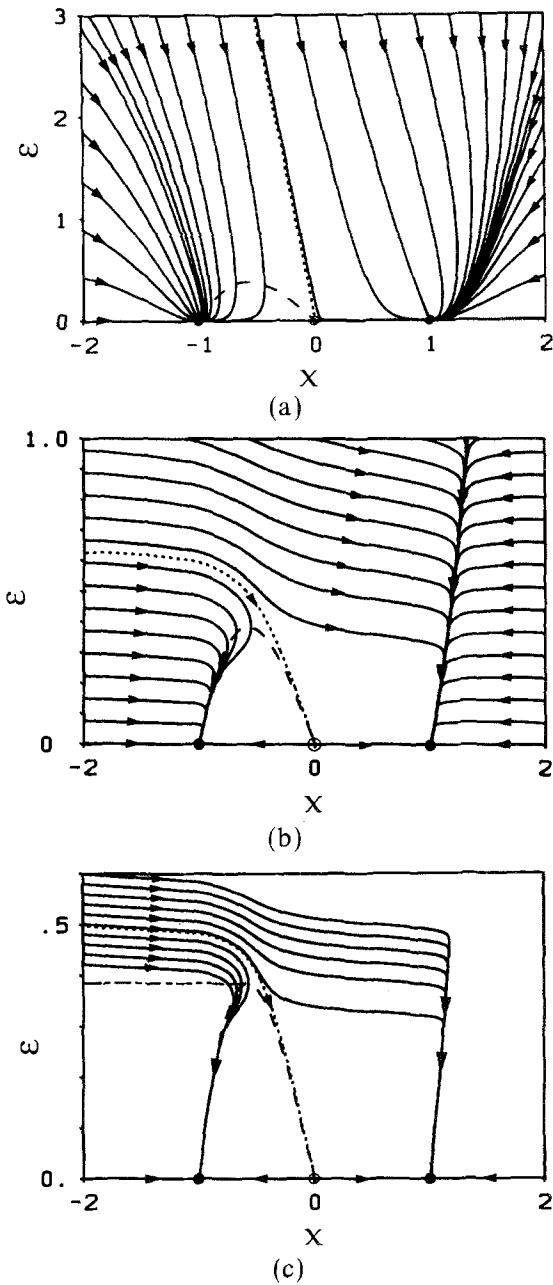


Fig. 1. Trajectories of the deterministic system (2.1) with the separatrix $\varepsilon_S(x)$ (dotted line) and the nodal curve $\varepsilon_T(x)$ (2.4) (dashed line); (a) $\tau = 0.2$, (b) $\tau = 10$, and (c) $\tau = 30$. In (c) the asymptotic curve $\varepsilon_S(x, \tau \rightarrow \infty)$, (2.7), is also drawn (dashed dotted).

attraction is indicated by a dotted line. The flow lines exhibit turning points, characterized by

$$d\varepsilon/dx = \infty \tag{2.2}$$

In view of the identities

$$\dot{x} = x - x^3 + \varepsilon = \frac{dx}{d\varepsilon} \frac{d\varepsilon}{dt} = -\frac{1}{\tau} \varepsilon \frac{dx}{d\varepsilon} \tag{2.3}$$

the sequence of turning points $\{dx/d\varepsilon = 0\}$ forms a nodal curve $\varepsilon_T(x)$ given by

$$\varepsilon_T(x) = x^3 - x \tag{2.4}$$

ε_T approaches a local maximum at

$$(x_c, \varepsilon_c) = \left(-\frac{1}{\sqrt{3}}, +\frac{2}{3\sqrt{3}} \right) \tag{2.5}$$

with a corresponding local minimum at $(-x_c, -\varepsilon_c)$. With τ being extremely large, we note that a particle moves *rapidly* toward the curve $\varepsilon_T(x)$ and then relaxes to the corresponding stable fixed point. The separatrix $\varepsilon_s(x, \tau)$ itself cannot be simply expressed in closed analytical form. Near the saddle point $(x = 0, \varepsilon = 0)$, a linearization scheme yields for the slope $d\varepsilon_s(x, \tau)/dx \equiv S(x; \tau)$ at $x = 0$ the result

$$S(0; \tau) = -(1 + 1/\tau) \tag{2.6}$$

The separatrix $\varepsilon_s(x; \tau)$ thus approaches the axis $x = 0$ for $\tau \rightarrow 0$ with a slope $S(0; \tau) \rightarrow -1/\tau$, whereas $S(0; \tau) \rightarrow -1$ as $\tau \rightarrow \infty$. In the limit $\tau \rightarrow \infty$, $\varepsilon_s(x; \tau)$ exhibits a cusp at $x = \pm x_c$ (see Fig. 1c), i.e.,

$$\lim_{\tau \rightarrow \infty} \varepsilon_s(x; \tau) = \left\{ \begin{array}{ll} \frac{2}{3\sqrt{3}}; & x \leq -\frac{1}{\sqrt{3}} \\ x^3 - x; & -\frac{1}{\sqrt{3}} < x < \frac{1}{\sqrt{3}} \\ -\frac{2}{3\sqrt{3}}; & x \leq -\frac{1}{\sqrt{3}} \end{array} \right\} \tag{2.7}$$

3. STATIONARY PROBABILITY

For Markovian flows of dimension $d \geq 2$ without detailed balance the solution for the stationary probability $\bar{p}(x, \varepsilon)$ is nontrivial; moreover, the

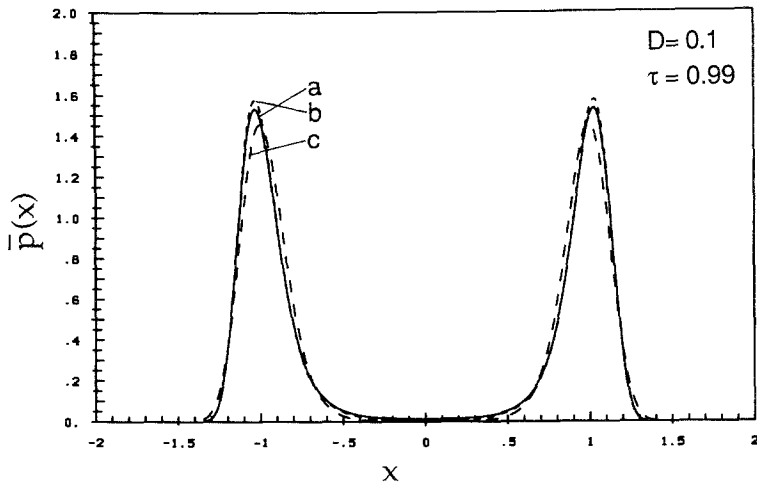


Fig. 2. Stationary distribution for the double-well potential with $D=0.1$ and $\tau=0.99$: (a) numerical results (error magnitude within line thickness), (b) UCNA prediction (3.5), (c) decoupling theory⁽²⁰⁾ prediction.

corresponding two-dimensional Fokker-Planck operator is not symmetric. Generally, there does not even exist a globally differentiable weak noise potential.⁽⁸⁻¹⁰⁾ In practice, the stationary x probability $\bar{p}(x; \tau) = \int \bar{p}(x, \varepsilon; \tau) d\varepsilon$ must be either evaluated numerically or within a suitable approximation. The stationary probability $\bar{p}(x; \tau)$ for the process (1.3) has been evaluated numerically by use of an improved matrix continued fraction method.⁽¹¹⁾ In Figs. 2 and 3 we display our results for $\bar{p}(x; \tau)$

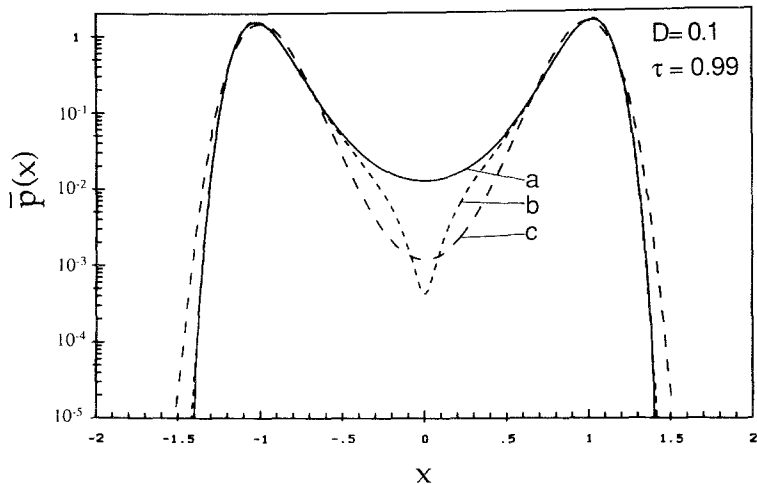


Fig. 3. Logarithmic plot of curves (a)-(c) in Fig. 2.

at $D = 0.1$ and $\tau = 0.99$. It has been shown that the choice of a suitable form function $\rho_0(x) = \exp(-cx^2)$ considerably improves the rate of the convergence of the conventional matrix-continued fraction algorithm pioneered by Risken and Vollmer⁽¹²⁾ and applied to various colored noise phenomena by Jung and Risken.^(13,14)

A useful approximation scheme for the dynamics in (1.3) is the unified colored noise approximation (UCNA).^(15,16) Upon elimination of $\varepsilon(t)$ in (1.3a) with the help of (1.3b) one obtains for (1.1) the flow of a nonlinear oscillator, i.e.,

$$\ddot{x} + \dot{x} \left[\frac{1}{\tau} - (1 - 3x^2) \right] - \frac{1}{\tau} (x - x^3) = \frac{D^{1/2}}{\tau} \xi(t) \tag{3.1}$$

By use of the new time scale $t = \tau^{1/2} \hat{t}$, we can recast (3.1) in the form

$$\ddot{x} + \gamma(x, \tau) \dot{x} - (x - x^3) = D^{1/2} \xi(\tau^{1/2} \hat{t}) \tag{3.2}$$

with

$$\gamma(x, \tau) = \tau^{-1/2} + \tau^{1/2} (-1 + 3x^2) \tag{3.3}$$

In regions of x space for which $\gamma(x, \tau) > 0$, the nonlinear damping approaches infinity both for $\tau \rightarrow 0$ and $\tau \rightarrow \infty$. Neglecting for large τ the velocity variations (i.e., $\ddot{x} = 0$), we find that the non-Markovian flow in (1.1) is approximated by a truly one-dimensional Markovian process obeying the (Stratonovich) stochastic differential equation⁽¹⁵⁾

$$\dot{x} = \gamma^{-1}(x, \tau)(x - x^3) + \tau^{-1/4} D^{1/2} \gamma^{-1}(x, \tau) \xi(\hat{t}) \tag{3.4}$$

with $\langle \xi(\hat{t}) \xi(\hat{t}') \rangle = 2\delta(\hat{t} - \hat{t}')$.

The corresponding approximate stationary probability $\bar{p}^{UCNA}(x; \tau)$ is readily obtained as⁽¹⁵⁾

$$\begin{aligned} \bar{p}^{UCNA}(x; \tau) = Z^{-1} & |1 - \tau(1 - 3x^2)| \exp \left[-\frac{\tau}{2D} (x - x^3)^2 \right] \\ & \times \exp \left[-\frac{1}{D} \left(\frac{x^4}{4} - \frac{x^2}{2} \right) \right] \end{aligned} \tag{3.5}$$

This result precisely coincides with the stationary probability obtained with the small- τ theory by Fox.⁽¹⁷⁾ However, the relevant Fokker-Planck equation corresponding to (3.4) distinctly differs from the effective Fokker-Planck approximation in ref. 17. For $\tau < 1$, $\bar{p}^{UCNA}(x; \tau)$ has a support extending over the whole real axis. For $\tau > 1$, however, the

approximation fails to describe the exact probability $\bar{p}(x, \tau)$ in the region of exponentially small but finite weight characterized by

$$|x| < |x_s| \equiv \left(\frac{\tau - 1}{3\tau} \right)^{1/2}, \quad \tau > 1 \quad (3.6)$$

Note that x_c [see (2.5)] always lies inside the support of $\bar{p}(x; \tau)$, i.e., $|x_c| > |x_s|$ for any value of τ . Apart from this region of no support, the UCNA provides a very accurate approximation to the exact probability, even for noise correlation times τ of order one (see Fig. 3) where $\gamma(x, \tau)$ is not extremely large. The result in (3.5) forms the key input for the calculation of the escape time T at large noise color $\tau \rightarrow \infty$.

Before we proceed in discussing the escape path for strongly correlated noise, we take a look at the two-dimensional stationary probability $\bar{p}(x, \varepsilon)$.^(2,14,18) The two-dimensional landscape provides further insight for the escape mechanism from one domain of attraction to the other. For small values of τ the point $(x=0, \varepsilon=0)$ is a *saddle point* of the two-dimensional probability and the most probable escape path crosses through this point. A recent discovery by Moss⁽¹⁹⁾ by means of analog simulation has demonstrated the possibility of the existence of a critical correlation time value τ_0 , at which the topology of the two-dimensional stationary probability changes qualitatively. For values of τ larger than the critical value τ_0 the point $(x=0, \varepsilon=0)$ is *no longer a saddle point*, but rather becomes a *local minimum* of the probability distribution. Thus, the escape paths mostly avoid the region around $(x=0, \varepsilon=0)$, i.e., escape takes place at larger values of ε .

In the following we derive an expression for the critical value τ_0 above which the point $(x=0, \varepsilon=0)$ is a minimum of the two-dimensional probability. All symmetric potentials $U(x)$ that admit at $x=0$ a maximum with nonvanishing curvature can be represented by studying the archetypal form $V(x) = -(a/2)x^2 + (b/4)x^4$. The two-dimensional stationary probability \bar{p} obeys the Fokker-Planck equation

$$-\frac{\partial}{\partial x} (ax - bx^3) \bar{p} - \frac{\partial}{\partial x} \varepsilon \bar{p} + \frac{1}{\tau} \frac{\partial}{\partial \varepsilon} \varepsilon \bar{p} + \frac{D}{\tau^2} \frac{\partial^2}{\partial \varepsilon^2} \bar{p} = 0 \quad (3.7)$$

The statistical potential $\phi(x, \varepsilon)$ defined by

$$\bar{p}(x, \varepsilon) \equiv \exp(-\phi(x, \varepsilon)) \quad (3.8)$$

obeys

$$(ax - bx^3 + \varepsilon) \frac{\partial \phi}{\partial x} + \frac{1}{\tau} - (a - 3bx^2) - \frac{1}{\tau} \varepsilon \frac{\partial \phi}{\partial \varepsilon} - \frac{D}{\tau^2} \frac{\partial^2 \phi}{\partial \varepsilon^2} + \frac{D}{\tau^2} \left[\frac{\partial \phi}{\partial \varepsilon} \right]^2 = 0 \quad (3.9)$$

Unfortunately, an expansion of $\phi(x, \varepsilon)$ into powers of x and ε does not lead to a closed system of equations for the corresponding expansion coefficients. An exception is the linear case ($b = 0$). Nevertheless, it is possible to show the transition from a saddle point to a minimum. Inserting the expansion

$$\phi(x, \varepsilon) = \alpha x^2 + \beta \varepsilon^2 + \gamma x \varepsilon \quad (3.10)$$

into (3.9) and comparing powers of x^0 and x^2 , one obtains

$$\beta = \frac{1}{2D} \tau(1 - a\tau) \quad (3.11a)$$

$$2a\alpha + 3b + \frac{D}{\tau^2} \gamma^2 = 0 \quad (3.11b)$$

The condition for $(x=0, \varepsilon=0)$ to be a saddle point (local minimum) is a positive (negative) discriminant of (3.10), $\Delta(\tau) = \gamma^2 - 4\alpha\beta$. Using (3.11), one finds

$$\Delta(\tau) = -\frac{\tau}{D} (2\alpha + 3b\tau) \quad (3.12)$$

The critical value τ_0 follows from the identity $\Delta(\tau_0) = 0$, i.e.,

$$\tau_0 = 2 \frac{|\alpha|}{3b} = \frac{1}{a} + \frac{D}{3b\tau_0^2 a} \gamma^2(\tau_0) \geq \frac{1}{a} \quad (3.13)$$

This relation shows the existence of a noise color-induced “saddle \rightarrow minimum” transition of $\bar{p}(x, \varepsilon)$. The quantity γ^2 can be calculated explicitly only in the linear approximation ($b = 0$), yielding $\gamma_{\text{lin}} = a(\tau/D)(1 - a\tau)$. Substituting γ^2 with γ_{lin}^2 in (3.13), we obtain for small D an approximate expression for τ_0 , i.e.,

$$\tau_0 = \frac{1}{a} + \frac{3Db}{a^3} \quad (3.14)$$

4. ESCAPE TIME FOR STRONG NOISE COLOR

Recalling the flow dynamics depicted in Figs. 1a–1c, we note that for τ large the particle moves rapidly into the neighborhood of the nodal curve $\varepsilon_T(x)$, (2.4), and then relaxes toward the corresponding stable node at $x = \pm 1$. Conversely, for a particle starting at $x = -1$, its escape route closely follows for $\tau \gg 1$ the line $\varepsilon_T(x)$ up to the maximum at (x_c, ε_c) .

Moreover, the region of (x, ε) values bounded by the line $\varepsilon=0$ and the nodal curve $\varepsilon_\tau(x)$ is visited only very rarely. *The crossing of the separatrix $\varepsilon_S(x; \tau)$ thus occurs as $\tau \rightarrow \infty$ most likely within the immediate neighborhood of (x_c, ε_c) .* Clearly, with τ assuming small to moderate values, there exist other escape paths which cross the separatrix at values of x much closer to the saddle point. At finite τ , the distance of (x_c, ε_c) from the separatrix $\varepsilon_S(x; \tau)$ is finite {e.g., $[\varepsilon_S(x_c, \tau=30) - \varepsilon_c]/\varepsilon_c \cong 0.17$ }. Therefore, with τ large but finite, the time $T(-1; \tau)$ to reach the point (x_c, ε_c) starting from $x = -1$ always *underestimates* the exact escape time (i.e., its reciprocal overestimates the exact escape rate).

For very large τ , the asymptotic behavior of the exact escape time is estimated with the mean first passage time (MFPT) for the spatial variable $x(t)$ in (3.4), to reach the critical value $x_c = -1/\sqrt{3}$, when it started at $x = -1$. With $x \rightarrow -\infty$ being a natural reflecting boundary, the MFPT, $T^{\text{UCNA}}(-1, \tau)$, for the Fokker-Planck process in (3.4) is given by⁽⁷⁾

$$T^{\text{UCNA}}(-1, \tau) = \int_{-1}^{-1/\sqrt{3}} \frac{dx}{D(x) p^{\text{UCNA}}(x)} \int_{-\infty}^x p^{\text{UCNA}}(y) dy \quad (4.1)$$

where [see Eq. (3.4)]

$$D(x) = D(1 + \tau(3x^2 - 1))^{-2} \quad (4.2)$$

Hereby, we already have expressed the escape time in the original, unscaled time variable, i.e., $T(-1, \tau) = \tau^{1/2} \hat{T}(-1, \tau)$. For weak noise $D \ll 1$, the second integration in (4.1) can be evaluated within a steepest descent approximation

$$T^{\text{UCNA}}(-1, \tau) \sim [\pi D(1 + 2\tau)]^{1/2} \exp\left(\frac{1}{4D}\right) \int_{-1}^{-1/\sqrt{3}} \frac{dx}{D(x) p^{\text{UCNA}}(x)} \quad (4.3)$$

The integral in (4.3) is dominated by values at the upper boundary $x \sim x_c = -1/\sqrt{3}$. The diffusion is slowly varying compared to the inverse of $p^{\text{UCNA}}(x)$. Setting $D(x) \rightarrow D(x_c) = D$, we obtain

$$T^{\text{UCNA}}(-1, \tau) \approx \left[\frac{\pi}{D}(1 + 2\tau)\right]^{1/2} \exp\left(\frac{1}{4D}\right) \int_{-1}^{-1/\sqrt{3}} \frac{dx}{p^{\text{UCNA}}(x)} \quad (4.4)$$

With an exponential first-order approximation to the integral in (4.4) at $x = x_c$ we find for the large- τ asymptotics at weak noise

$$T^{\text{UCNA}}(-1, \tau \rightarrow \infty) \sim \left[\frac{27}{2} \pi D \left(\tau + \frac{1}{2}\right)\right]^{1/2} \exp\left[\frac{1}{4D} \left(\frac{4}{9} + \frac{8}{27} \tau\right)\right] \quad (4.5a)$$

In terms of the unscaled variables [see (1.1)] this result reads

$$T^{\text{UCNA}}(-1, \tau \rightarrow \infty) \sim \left[\frac{27\pi D}{8V_0 a^2} \left(a\tau + \frac{1}{2} \right) \right]^{1/2} \exp \left[\frac{V_0}{D} \left(\frac{4}{9} + \frac{8}{27} a\tau \right) \right] \quad (4.5b)$$

where $V_0 = a^2/4b$ denotes the barrier height.

This asymptotic result can now be compared with the exact numerical calculations for the smallest nonvanishing eigenvalue $\lambda_1(\tau)$ of the nonsymmetric Fokker–Planck operator corresponding to the *two-dimensional* Markovian dynamics in (1.3). Such an eigenvalue is (at weak noise) related to the rate of escape $\Gamma(\tau)$ by $\Gamma(\tau) = 1/[2T(-1; \tau)] = \lambda_1(\tau)/2$. Jung and Hänggi⁽¹¹⁾ have recently performed these detailed calculations using an improved matrix continued fraction method. $\lambda_1(\tau)$ turns out to be real for all values of τ considered. The precise numerical results for $\lambda_1(\tau)$ are

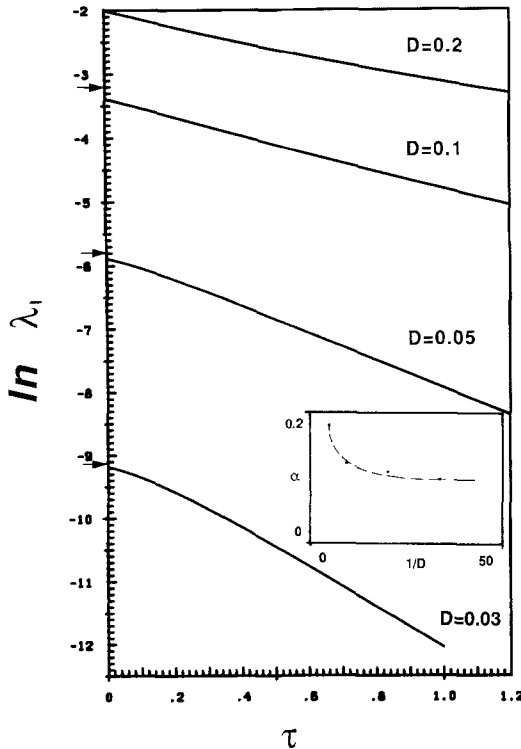


Fig. 4. Eigenvalues (numerical error <0.1%) of the two-dimensional Fokker–Planck operator corresponding to (1.3). The arrows indicate the eigenvalues for $\tau=0$, calculated approximately with the steepest descent method. The inset shows the D dependence of α [see Eq. (4.7)].

plotted in Fig. 4 at various weak noise intensities for small to moderate noise color, being the physically relevant regime of correlated noise. For very small noise color we observe a behavior of the form⁽¹¹⁾

$$\lambda_1(\tau) = \lambda(0)[1 - \beta(D)\tau], \quad \tau \rightarrow 0, \quad \tau/D \ll 1 \quad (4.6)$$

with a weakly D -dependent β value ($\beta = 1.33$ at $D = 0.05$; $\beta = 1.44 \pm 0.02$ at $D = 0.03$). We note that the domain of validity of the small- τ behavior (4.6) gets smaller with decreasing D ; this is in contrast to the familiar argumentation given for the small- τ theories that $D\tau$ alone is a small quantity. Outside this small- τ domain, there occurs an interesting but complex crossover to a behavior for moderate $\tau \sim O(1)$ that is well represented by an exponential law of the form⁽¹¹⁾

$$\lambda_1(\tau) \propto \exp(-\alpha\tau/D), \quad \tau > 0.2 \quad (4.7)$$

The weakly D -dependent coefficient α is shown in the inset of Fig. 4. The behavior in (4.7) is in qualitative agreement with the decoupling theory.^(16,20-22) For small D , and $\tau \sim O(1)$, we find $\alpha \cong 0.1$, whereas the result in (4.5a) predicts a value $\alpha_{as} = \lim_{\tau \rightarrow \infty} \lim_{D \rightarrow 0} D d[\ln T(\tau)]/d\tau$, which reads³

$$\alpha_{as} = 2/27 = 0.074, \quad a = b = 1 \quad (4.8)$$

It must be emphasized, however, that for weak noise a small error in the coefficient α affects significantly the value of the slope of $-d \ln \lambda_1(\tau)/d\tau$; i.e., a minor error in α strongly enhances the error for the escape rate $\Gamma(\tau) = \lambda_1(\tau)/2$.

The asymptotic result in (4.5) with $\lambda^{\text{UCNA}}(\tau) \equiv [T^{\text{UCNA}}(-1, \tau)]^{-1}$ is compared in Fig. 5 with the numerical results ($D = 0.05$) at small to moderate noise color $\tau \leq 1.3$. As is evident, the result in (4.5) is indeed an asymptotic one: Although the slopes of the two curves are quite close, the value of $\lambda_1(\tau)$ itself slowly approaches the exact result (4.5), valid at large τ .

³ This asymptotic result has also been derived by Luciani and Verga.^(23,24) These authors employ path integral techniques for a bistable system with a piecewise linear flow. If their results are adapted to our Ginzburg-Landau flow in (1.3a), one finds from their Eq. (66) in ref. 24 that

$$T(\tau) = \pi \left(\frac{3}{2} \tau \right)^{1/2} \exp \left[\frac{1}{4D} \left(\frac{8}{27} \tau + \frac{601}{729} + \frac{2048}{19683} \tau^{-1} \right) \right] \quad \text{as } \tau \rightarrow \infty$$

i.e., $\alpha_{as} = 2/27$. This same asymptotic value for α_{as} has been found later by Tsironis and Grigolini⁽²⁵⁾ using an adiabatic potential argument. If we set $T(\tau) \propto \exp[(1/4D)(4\alpha_{as}\tau + \kappa)]$, as $\tau \rightarrow \infty$, we find in this work $\kappa = 4/9 \approx 0.44$; Luciani and Verga obtain $\kappa = 601/729$ and Tsironis and Grigolini have $\kappa = 0$.

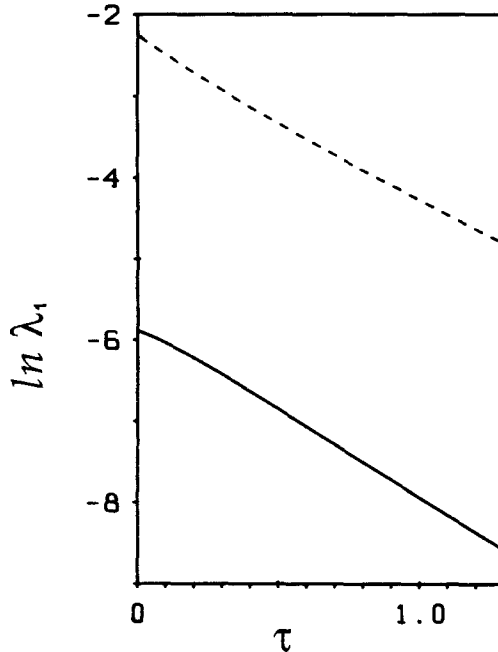


Fig. 5. Comparison of the numerical result for the smallest eigenvalue $\lambda_1(\tau)$ (error $< 0.1\%$) (solid line) with the asymptotic prediction (dashed line) (4.5) for $D = 0.05$.

Accurate calculations of the smallest eigenvalue $\lambda_1(\tau)$ for $\tau \gg 1$ and at weak noise, however, are beyond our computational possibilities.

5. CONCLUSIONS

In the preceding sections we have focused our investigation on the influence of strong noise color in the bistable dynamics in (1.1). The main results have been the form of the separatrix as $\tau \rightarrow \infty$, (2.7), the noise-color-induced “saddle \rightarrow minimum transition” of \bar{p} at a critical value τ_0 [see Eq. (3.14)], and the asymptotic expression for the escape time in (4.5). Evidence for the saddle–minimum transition has been recently produced by analog simulations.⁽¹⁹⁾ Although the limiting behaviors for $\tau \rightarrow 0$, (4.6), and $\tau \rightarrow \infty$, (4.5), are interesting for themselves, the practice of colored noise phenomena^(1–4) generally dictates a parameter regime different from such asymptotic regimes. Typically, the noise intensity is rather weak [$D \sim O(10^{-2}–10^{-1})$] and the physical noise color amounts to dimensionless values of $O(10^{-1}–10)$. Thus, with $D \sim 10^{-2}$, the small- τ asymptotics in (4.6) limits the noise color to very small τ values, $\tau \ll 10^{-2}$.

Likewise, the large- τ asymptotics in (4.5) sets in only for $\tau \geq 10^2$ (see also Figs. 4 and 5). Although the decoupling theory⁽²⁰⁾ provides qualitatively correct insight in the intermediate regime, i.e., $\tau \sim O(1)$, we still lack a quantitative theory describing the numerical results.

A theory describing this very intermediate regime will be rather complex: With the noise color approaching finite values of order $O(1)$, the most likely escape paths shall deviate with decreasing $\tau \downarrow O(1)$ more and more from the nodal line given by (2.4). The most probable crossing point of the separatrix will be shifted toward smaller x values around $x \sim 0$. Put differently, the actual escape time becomes dressed by large-amplitude (path) fluctuations describing the deviation from the asymptotic escape path at $\tau \gg 1$. Thus, a more detailed quantitative theory (e.g., see refs. 23 and 24) modeling moderate noise color τ must account for these path fluctuations which modify the exponential part in (4.5), i.e., the coefficient α_{as} , as well as the prefactor.

The numerically established laws (4.6) and (4.7) have a limited range of validity in τ ; with (4.6) for $\tau \rightarrow 0$, (4.7) at moderate τ , and (4.5) as $\tau \rightarrow \infty$, there must exist at least two nontrivial crossover regimes. A first one describes a smooth crossover between $\tau \sim O(10^{-2})$ toward moderate values $\tau \sim O(1)$, while a second one must describe a slowly varying crossover from the behavior in (4.7) with $\alpha \sim 0.1$ toward the asymptotic regime with $\alpha = \alpha_{as} \sim 0.074$ as $\tau \rightarrow \infty$. For weak noise, this second crossover regime is characterized by a slow convergence to the limiting asymptotic law in (4.5); it implies a very small positive curvature in the plot of $\ln \lambda_1(\tau)$, $\tau \gg 1$, which in fact can be detected already in Fig. 4 with $D \geq 0.1$. This very same small positive curvature in $\ln \lambda_1(\tau)$ is also present in the numerical analysis of the colored-noise-driven dynamics in a periodic, multistable potential.⁽²²⁾

REFERENCES

1. P. Lett, R. Short, and L. Mandel, *Phys. Rev. Lett.* **52**:341 (1984); S. Zhu, A. W. Yu, and R. Roy, *Phys. Rev. A* **34**:4333 (1986); R. F. Fox and R. Roy, *Phys. Rev. A* **35**:1838 (1987).
2. K. Vogel, Th. Leibler, H. Risken, P. Hänggi, and W. Schleich, *Phys. Rev. A* **35**:4882 (1987); K. Vogel, H. Risken, W. Schleich, M. James, F. Moss, and P. V. E. McClintock, *Phys. Rev. A* **35**:463 (1987).
3. R. Kubo, in *Fluctuations, Relaxation and Resonance in Magnetic Systems*, D. ter Haar, ed. (Edinburgh University Press, 1962), pp. 23–68.
4. P. Hänggi, *J. Stat. Phys.* **42**:105 (1986); **44**:1003 (1986).
5. R. F. Grote and J. T. Hynes, *J. Chem. Phys.* **73**:2715 (1980); P. Hänggi and F. Mojtabai, *Phys. Rev. A* **26**:1168 (1982); B. Carmeli and A. Nitzan, *Phys. Rev. A* **29**:1481 (1984); J. E. Straub, M. Borkovec, and B. J. Berne, *J. Chem. Phys.* **84**:1788 (1986); R. Zwanzig, *J. Chem. Phys.* **86**:5801 (1987); P. Talkner and H. B. Braun, *J. Chem. Phys.* **88**:7537 (1988).

6. N. G. Van Kampen, *Physica* **23**:707, 816 (1957); U. Uhlhorn, *Arch. Physik* **17**:361 (1960); R. Graham, *Z. Physik B* **40**:149 (1980); P. Hänggi, *Phys. Rep.* **88C**:207 (1982), pp. 265–274.
7. P. Hänggi, F. Marchesoni, and P. Grigolini, *Z. Physik B* **56**:333 (1984).
8. M. I. Freidlin and A. D. Wentzell, *Random Perturbations of Dynamical Systems* (Springer, Berlin, 1984).
9. R. Graham and T. Tel, *J. Stat. Phys.* **35**:729 (1984); *Phys. Rev. A* **31**:1109 (1985).
10. H. R. Jauslin, *J. Stat. Phys.* **42**:573 (1986); *Physica* **144A**:179 (1987).
11. P. Jung and P. Hänggi, *Phys. Rev. Lett.* **61**:11 (1988).
12. H. Risken and H. D. Vollmer, *Z. Phys. B* **33**:297 (1979); H. Risken, *The Fokker–Planck Equation* (Springer, Berlin, 1984).
13. P. Jung and H. Risken, *Phys. Lett. A* **103**:38 (1984).
14. P. Jung and H. Risken, *Z. Physik B* **61**:367 (1985).
15. P. Jung and P. Hänggi, *Phys. Rev. A* **35**:4464 (1987).
16. P. Jung and P. Hänggi, *J. Opt. Soc. Am. B* **5** (1988).
17. R. F. Fox, *Phys. Rev. A* **33**:467 (1986); **34**:4525 (1986); **37**:911 (1988); *J. Stat. Phys.* **46**:1145 (1987).
18. F. Moss and P. V. E. McClintock, *Z. Physik B* **61**:381 (1985).
19. F. Marchesoni and F. Moss, *Phys. Lett. A* **131**:322 (1988); F. Moss, private communication.
20. P. Hänggi, T. J. Mroczkowski, F. Moss, and P. V. E. McClintock, *Phys. Rev. A* **32**:695 (1985).
21. F. Marchesoni, *Phys. Rev. A* **36**:4050 (1987).
22. Th. Leibler, F. Marchesoni, H. Risken, *Phys. Rev. Lett.* **59**:1381 (1987).
23. J. F. Luciani and A. D. Verga, *Europhys. Lett.* **4**:255 (1987).
24. J. F. Luciani and A. D. Verga, *J. Stat. Phys.* **50**:567 (1988).
25. G. Tsironis and P. Grigolini, *Phys. Rev. Lett.* **61**:7 (1988).